# X-ray Spectroscopy:
# What it has told us & what we will learn in future


**Ken Phillips**

*Scientific Associate*
*Earth Sciences Department*
*Natural History Museum, London*
*London SW7 5BD, UK*

# A short history of X-rays

Discovered in 1895 by Wilhelm Röntgen using fluorescent tubes – they passed through human flesh & you could see bones.

*Image of Bertha Röntgen's hand*

Max von Laue discovered the diffraction of X-rays in crystals in 1912. Opened the field to William Henry and William Lawrence Bragg – WLB formulated the famous Bragg's law

$$\lambda = 2d \sin \theta$$

for 1st-order diffraction in a crystal where the separation of the planes is *d* and the angle of incidence is $\theta$.

*M. von Laue*

X-ray beam

Crystal planes

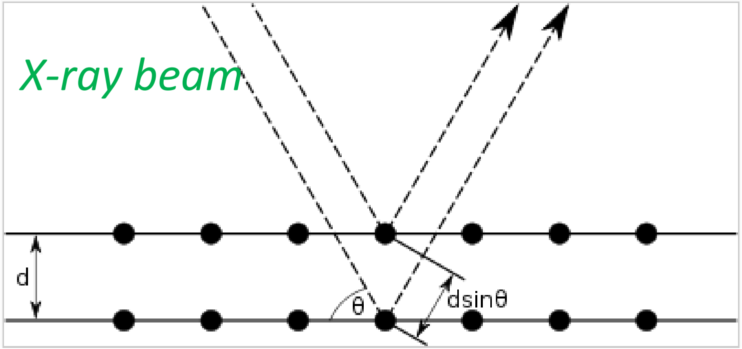

# More on Bragg's equation

W. L. Bragg won the Nobel Prize for Physics in 1915 and was until recently the youngest Nobel Prize winner ever. He became a famous TV broadcaster. His daughter Patience Thomson is still alive & "endorsed" my quotation of her father's equation a few weeks ago.

**Figure 1**
Together with my father in 1943.



BCS count rates that a flare was in progress. First, a 4′×4′ raster scan of the now flaring region was performed; this raster shows the same X-ray feature as earlier but with increased intensity. The FCS was then repointed at the point of greatest emission in the S XV line (home position line for channel 5), and short-wavelength regions covering the home position lines were scanned eight times between 1307 and 1310 UT. Each scan was performed by rotating the crystals in 30″ increments and collecting data for 0.512 s at each point. Light curves obtained with the BCS show that, by the start of these wavelength scans, the high-temperature line emission had already started to decline (Ca XIX maximum was at 1306 UT), although emission in the low-energy channels of the FCS was still increasing. The crystals were then driven to their minimum wavelength positions, and a continuous scan (in 50″ increments, 0.512 s at each point) was performed to the opposite end, this taking 17.5 minutes (1310–1328 UT). By the start of this long scan, the BCS Ca XIX flux had decreased to 70% of its maximum value, while by the end of the scan the emission was only 25% of this value.

The decrease in flare intensity is indicated by generally decreasing line intensities over the scan, but fortunately lines from highest temperature ions (Fe XXIII, etc.) present in the spectra occur at the start of the scan (in channel 2), so these lines are visible. A large pseudo-continuum level, partly instrumental in origin, is visible over the whole scan but also decreases with time. The exact causes of this pseudo-continuum are still under study, but meanwhile it has been subtracted in order to analyze line intensities.

From *Solar-Geophysical Data*, the H$\alpha$ flare on November 5 was appreciably larger (importance 1B) than the August 25 flare. It occurred in NOAA region 2776, with start and maximum times at 2226 and 2234 UT, and lasted for at least an hour after maximum. On this occasion, the FCS preplanned sequence was triggered by a flare flag at 2226 UT from the Hard X-ray Imaging Spectrometer (HXIS) on *SMM*. The FCS response was then 2′×2′ rasters, centered on the HXIS flare location. Checks were made by the FCS microprocessor to see whether the emission was sufficiently bright in Fe XXV (channel 7 home position), and, when this condition was satisfied, the FCS repointed at the

showed an initial decline and a subsequent large rise, with maximum at the start of the longer scans. The six scans were then repeated between 2245 and 2300 UT. The light curves of lines as seen with the FCS show that the flare was still in progress at 2300 UT.

The spectral scans on September 23 were over particular, active region lines of interest, e.g., lines due to Fe XVII, O VII, and Ne X. At the time (about 2010 UT), the active region was not flaring, and the FCS sequence was set off in a real-time pass of the spacecraft in order to obtain simultaneous coverage with a high-resolution X-ray grating experiment on board a rocket.

IV. WAVELENGTH DETERMINATIONS

Since the FCS spectra are of high quality, attempts were made to obtain line wavelengths to greatest possible accuracy. In this section, the procedure used for deriving wavelengths will be described; these wavelengths and line identifications will be discussed in § V.

The raw data for the FCS spectral scans consist of counts in 0.256 s intervals and crystal shaft addresses, as read from one of the drive-encoder units. Addresses increment by 1 for each step (9″.89), and so, for the full 28° rotation range of the shaft, there is an address range of about 10,200. Conversion of addresses to wavelengths is by Bragg's law of diffraction, modified for corrections due to X-ray refraction within the crystal. (For further details, see Compton and Allison 1935.)

Bragg's law for first-order diffraction of X-rays by a crystal (without refraction corrections) is

Patience Thomson.

$$\lambda = 2d \sin \theta_0 , \tag{1}$$

where $d$ is the crystal plane spacing and $\theta_0$ a nominal glancing angle of incidence. This is corrected to

$$\lambda = 2d(1-\delta \operatorname{cosec}^2 \theta) \sin \theta \tag{2}$$

to allow for refraction, where $\theta$ is the actual glancing angle and $\delta$ is the unit decrement of refractive index $\mu(\delta = 1-\mu)$, a function of $\lambda$. The unit decrement $\delta$ was determined from values of refractive index correction $\Delta$, which were measured prelaunch at particular wavelengths, using

# X-ray Crystallography

von Laue's and Bragg's work on X-ray diffraction in crystals set off a huge new study called X-ray crystallography which continues to this day.

Memorable discoveries include Kathleen Lonsdale's discovery of the structure of benzene, Dorothy Hodgkin's discovery of the structure of the structure of penicillin, and most notably the structure of DNA (Rosalind Franklin, Wilkins, Crick & Watson) in the early 1950s.

*Largest model of the NaCl molecule in the world*

# Solar X-ray astronomy

First attempt to get X-ray emission from the Sun made by T. R. Burnight (1949) at US NRL with X-ray telescope on a rocket.

Early X-ray photographs (with film) made in the 1960s.

*Solar X-ray images in 1966 with telescope on an Aerobee rocket (Muney & Underwood)*

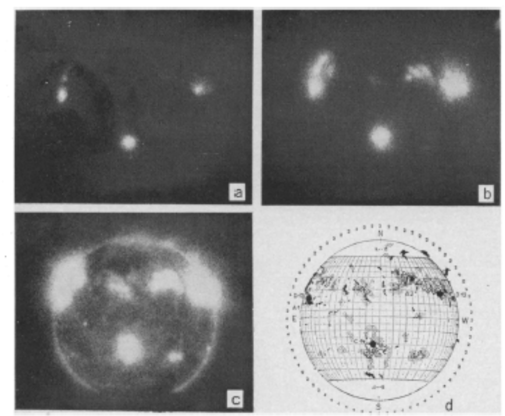


Fig. 5. X-ray photographs of the sun obtained on 20 May 1966. (a) Wavelength region 3–11 angstroms; (b) wavelength region 8–20 angstroms; (c) wavelength region 27–40 angstroms (contaminated by some radiation at 3–11 angstroms); (d) Fraunhofer Institut map of the sun for the same day.

There then followed several attempts to get X-ray spectra – first using proportional counters with crude spectral resolution, then with scanning crystals using the Bragg principle (varying the angle $\theta$ with time).

# Some early X-ray spectra during solar flares

Neupert et al. (1967) obtained spectra on OSO-3 (using a stepper motor to change the crystal angle θ) during a class 2b (Hα class). Their spectrum is one of the few to obtain X-ray line emission at very short wavelengths at this time.

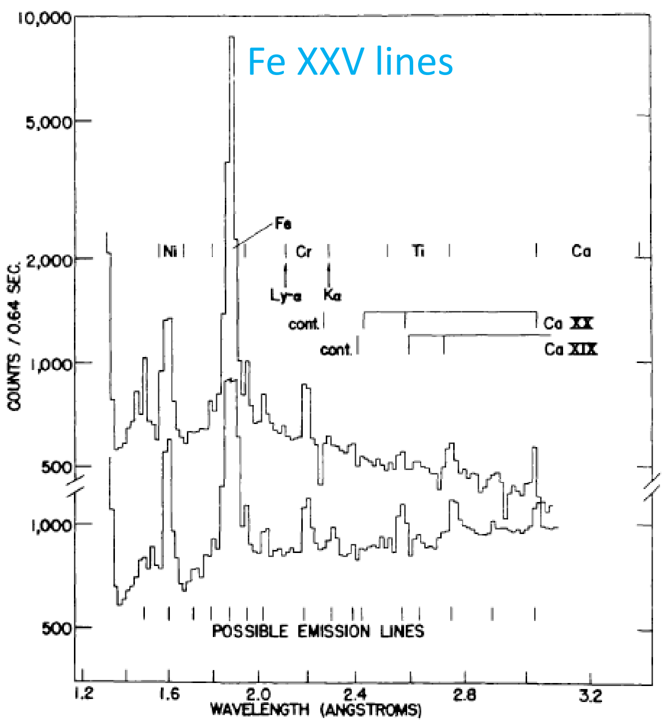


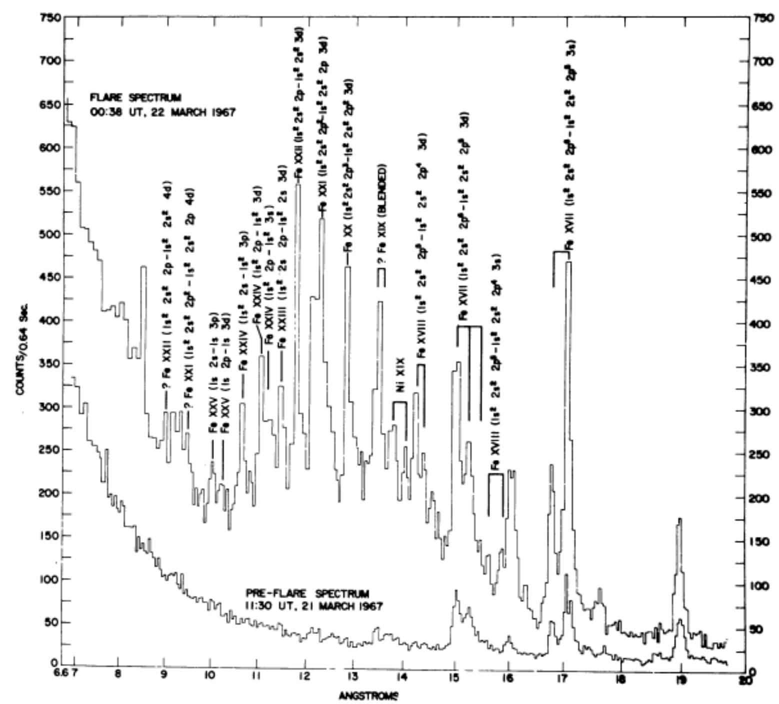

# Formation of X-ray lines

The ionization conditions in hot solar plasmas like flares are governed by collisional ionization and recombination by radiative and dielectronic processes.

For the He-like Fe ion – $Fe^{+24}$ – the main (resonance) line at 1.850 Å is excited by collisions with free electrons:

$Fe^{+24}(1s^2) + e^- \rightarrow Fe^{+24}(1s2p) + e^-$

$Fe^{+24}(1s2p) \rightarrow Fe^{+24}(1s^2) + h\nu$

where the photon $h\nu$ is an Fe XXV line w (wavelength of 1.850 Å).

Other Fe XXV lines are possible including the "forbidden" line ($1s2s \rightarrow 1s^2$) at 1.87 Å.

But there are numerous other lines, some intense, most hardly visible, which are due to dielectronic recombination.

# Dielectronic recombination

Dielectronic recombination is an “exotic” atomic process but it has great importance in the solar atmosphere.

By it, an ion such as $Fe^{+24}$ recombines to $Fe^{+23}$ by a sequence of processes:

$Fe^{+24} + e^{-} \rightarrow Fe^{+23**}$ (doubly excited Li-like Fe)

The reverse (“autoionization”) process: $Fe^{+23**} \rightarrow Fe^{+24} + e-$

may occur.

But also the doubly excited state may be “stabilized” by one or more “radiative” de-excitations.

Take the case of $Fe^{+23}$ (1s2s2p) (so two electrons excited to the n=2 shell).

Radiative de-excitation occurs by:

$Fe^{+23}$ (1s2s2p) $\rightarrow$ $Fe^{+23}$ ($1s^2$ 2s) + hν (X-ray satellite at 1.87 Å)

# Numerous X-ray lines formed

There are nearly endless possible transitions, for example:

$Fe^{+24} + e^{-} \rightarrow Fe^{+23}$ (1s 2p 5p)

$Fe^{+23}$(1s 2p 5p) $\rightarrow Fe^{+23}$ ($1s^2$ 5p)

or

$Fe^{+24} + e^{-} \rightarrow Fe^{+23}$ (1s 2p 12p)

$Fe^{+23}$(1s 2p 12p) $\rightarrow Fe^{+23}$ ($1s^2$ 12p) + $h\nu$

These lines are weak, but their "cumulative" effect is large – most of them "converge" on the Fe XXV resonance line.

# The 1.85 Å group of Fe X-ray lines

The 1.85 Å group of lines attracted much interest – they are due to He-like Fe formed at extremely high (T ~ 20MK) temperatures. Grineva et al. (1971, 1973) obtained high-resolution spectra during intense flares, as did Neupert & Swartz (1970) and Doschek et al. (1971). Much line structure which was soon interpreted as satellite lines.

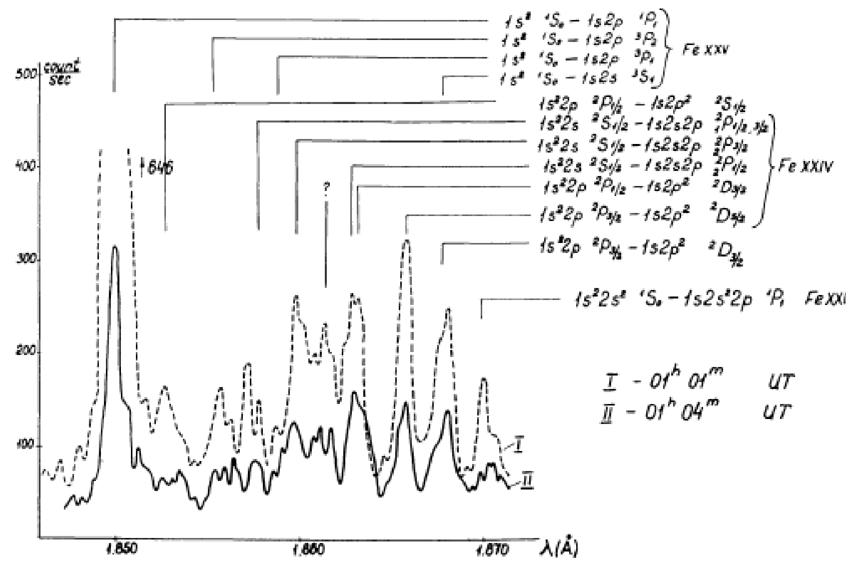


Fig. 1. Spectrum of the solar flare on 16 Nov. 1970. I – 01h01m UT; II – 01h04m UT.

*Academician S. L. Mandelstam*

# Fe (iron) satellite lines

Satellites were identified in laboratory spectra by Edlén and Tyrén (1939).

Theory of their formation worked out by Gabriel (1972). Here is a partial list of Fe XXIV satellites near 1.85 Å, showing 22 satellites:

Table 1. Wavelength and $F_2(S)$ for $n = 2$ satellites and Fe XXV lines (after Paper III).

*Fe XXIV satellites:*

| Array | Multiplet | Line | Key Letter | $\lambda$ (Å) | $F_2(S)$ $s^{-1}$ |
|---|---|---|---|---|---|
| $1s^2 2p-1s2p^2$ | $^2P^o-^2P$ | $1\frac{1}{2}-1\frac{1}{2}$ | a | 1.8615 | 1.21(14) |
| | | $\frac{1}{2}-1\frac{1}{2}$ | b | 1.8564 | 2.50(12) |
| | | $1\frac{1}{2}-\frac{1}{2}$ | c | 1.8667 | 4.13(11) |
| | | $\frac{1}{2}-\frac{1}{2}$ | d | 1.8616 | 1.41(12) |
| | $^2P^o-^4P$ | $1\frac{1}{2}-2\frac{1}{2}$ | e | 1.8725 | 8.03(13) |
| | | $1\frac{1}{2}-1\frac{1}{2}$ | f | 1.8747 | 4.86(12) |
| | | $\frac{1}{2}-1\frac{1}{2}$ | g | 1.8695 | 7.45(10) |
| | | $1\frac{1}{2}-\frac{1}{2}$ | h | 1.8771 | 3.94(9) |
| | | $\frac{1}{2}-\frac{1}{2}$ | i | 1.8719 | 3.82(11) |
| | $^2P^o-^2D$ | $1\frac{1}{2}-2\frac{1}{2}$ | j | 1.8653 | 5.13(14) |
| | | $\frac{1}{2}-1\frac{1}{2}$ | k | 1.8622 | 3.50(14) |
| | | $1\frac{1}{2}-1\frac{1}{2}$ | ℓ | 1.8674 | 3.36(13) |
| | $^2P^o-^2S$ | $1\frac{1}{2}-\frac{1}{2}$ | m | 1.8561 | 4.85(13) |
| | | $\frac{1}{2}-\frac{1}{2}$ | n | 1.8511 | 1.76(12) |
| $1s^2 2p-1s2s^2$ | $^2P^o-^2S$ | $1\frac{1}{2}-\frac{1}{2}$ | o | 1.8966 | 1.67(13) |
| | | $\frac{1}{2}-\frac{1}{2}$ | p | 1.8913 | 1.69(13) |
| $1s^2 2s-1s2p2s$ | $^2S-(^1P)^2P^o$ | $\frac{1}{2}-1\frac{1}{2}$ | q | 1.8601 | 3.08(11) |
| | | $\frac{1}{2}-\frac{1}{2}$ | r | 1.8631 | 6.73(13) |
| | $^2S-(^3P)^2P^o$ | $\frac{1}{2}-1\frac{1}{2}$ | s | 1.8558 | 1.68(13) |
| | | $\frac{1}{2}-\frac{1}{2}$ | t | 1.8562 | 1.09(14) |
| | $^2S-^4P^o$ | $\frac{1}{2}-1\frac{1}{2}$ | u | 1.8732 | 3.21(11) |
| | | $\frac{1}{2}-\frac{1}{2}$ | v | 1.8742 | 4.21(11) |

*Fe XXV lines:*

| Array | Multiplet | Line | Key Letter | $\lambda$ (Å) | $F_2(S)$ $s^{-1}$ |
|---|---|---|---|---|---|
| $1s^2-1s2p$ | $^1S-^1P^o$ | 0-1 | w | 1.8500 | - |
| | $^1S-^3P^o$ | 0-2 | x | 1.8550 | - |
| | | 0-1 | y | 1.8591 | - |
| $1s^2-1s2s$ | $^1S-^3S$ | 0-1 | z | 1.8678 | - |

# Theory of dielectronic satellites

The ratio of the intensity of a satellite line to the intensity of a resonance line ($I_{sat} / I_{res}$) depends on temperature:

$$\frac{I_{sat}}{I_{res}} \approx \frac{1}{T} A_a \frac{A_r}{A_a + \Sigma A_r}$$

where $T$ = electron temperature, $A_a$ = probability of auto-ionization, $A_r$ = probability of a radiative transition.

# Satellite lines & how to get temperature.

Now $A_a$ is approximately constant with atomic number $Z$ but $A_r$ varies at $Z^4$. Very roughly:

$$\frac{I_{sat}}{I_{res}} \approx \frac{1}{T} \times \frac{Z^4}{K + Z^4}$$

where $K$ = a constant.

So $I_{sat} / I_{res}$ depends on $1/T$, providing a very useful temperature "diagnostic".

For small Z, $I_{sat} / I_{res}$ increases at $Z^4$ and therefore the satellites of Fe XXIV ($Z$=26) are much more intense than Ne VIII ($Z$=10), and also even for Ca XVIII ($Z$=20).

# Solar flare spectra of Fe XXV lines and Fe XXIV satellites: observations by the BCS on the *SMM* spacecraft

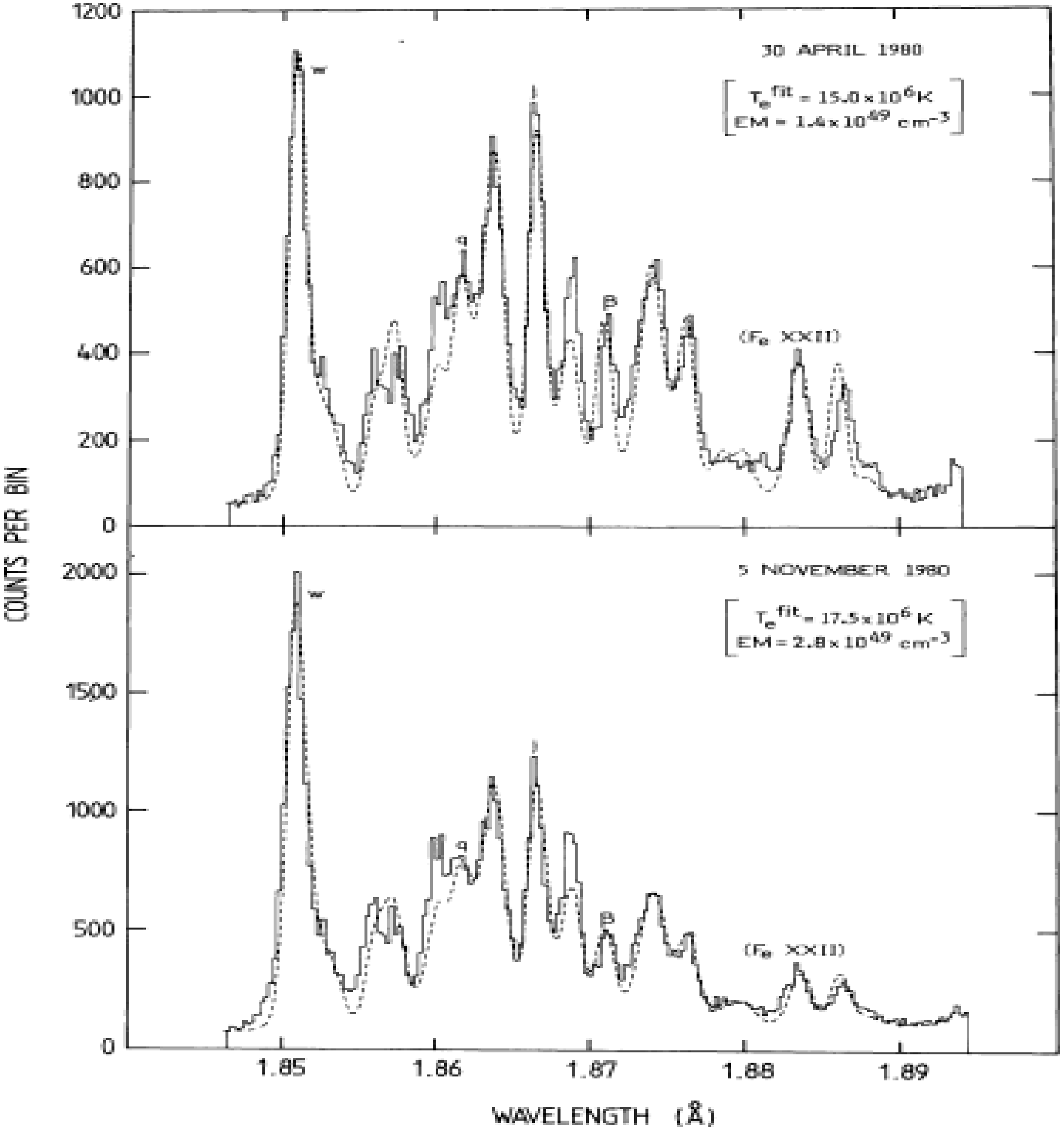


**$T_e$=15.0MK:**

**Satellites intense compared with Fe XXV resonance line w.**

**$T_e$=17.5 MK:**

**Satellites weaker compared with Fe XXV line w.**

*Lemen et al. (A&A1984)*

# Spectra from the *Hinotori* spacecraft

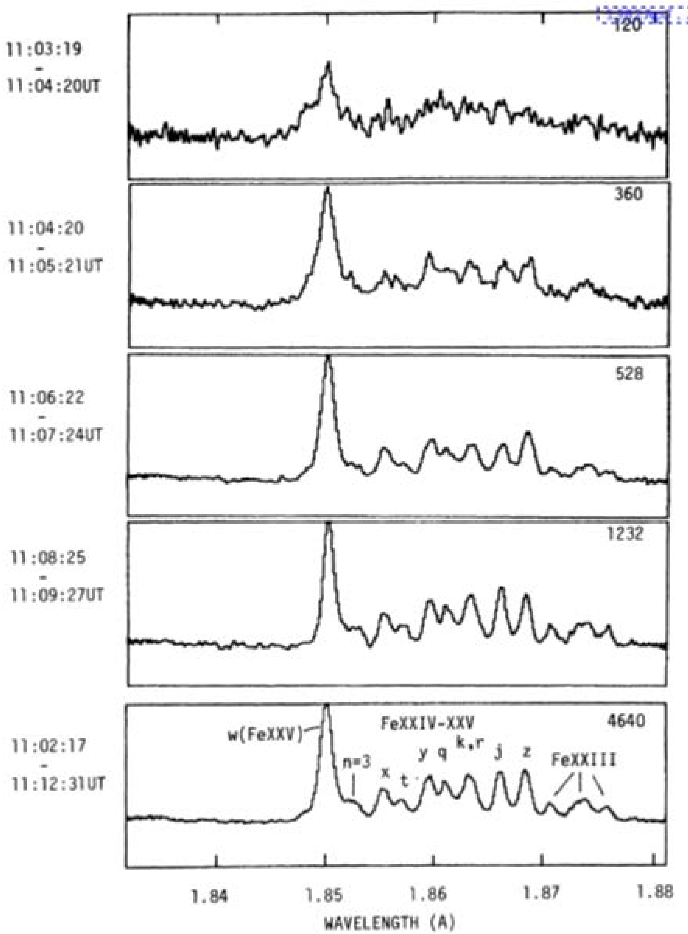


Fe XXV/Fe XXIV spectra of an intense flare obtained with the SOX2 spectrometer on the Japanese *Hinotori* spacecraft.

*Tanaka et al. (ApJ 1982)*

# Spectra from the P78-1 spacecraft

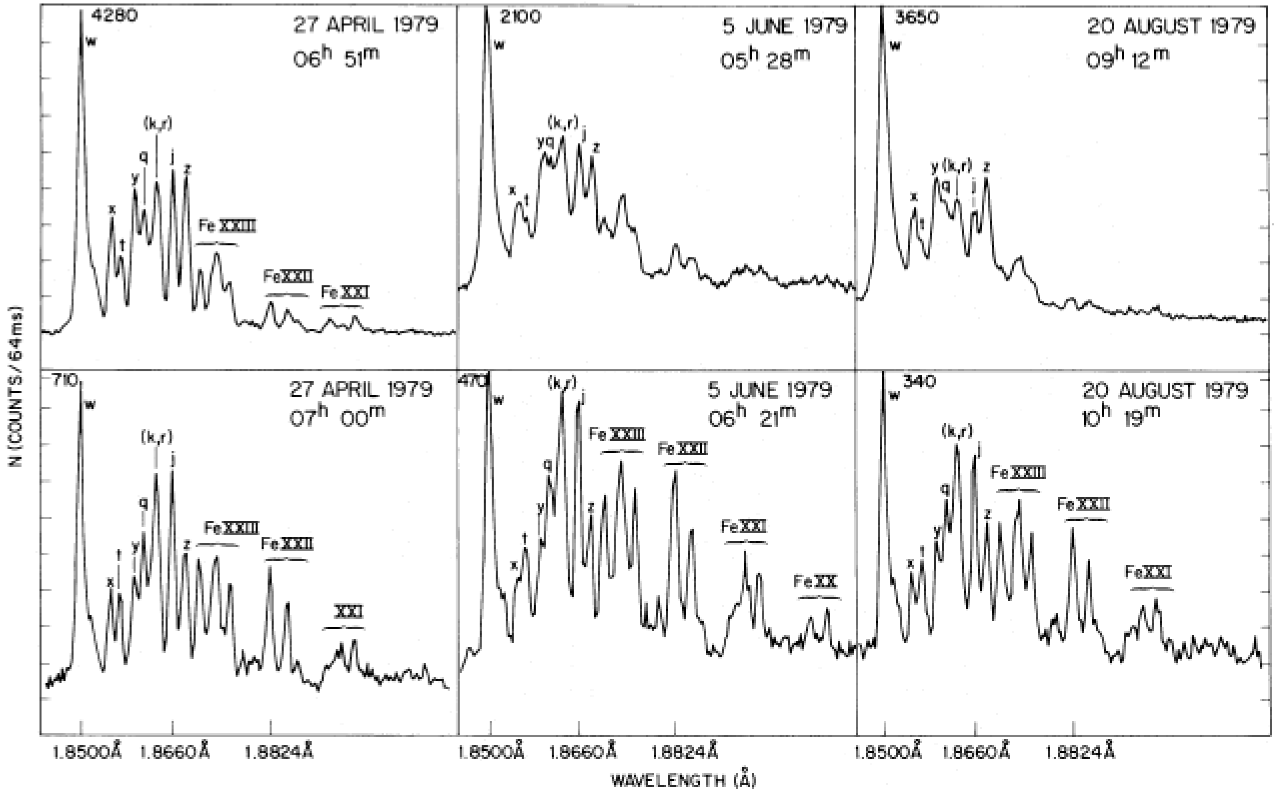


*Doschek et al. (ApJ 1980)*

Fe XXV/Fe XXIV spectra from 3 class X flares in 1979 seen with the SOLFLEX instrument on the US Air Force spacecraft *P78-1*.

# Fe XXV and Fe XXIV satellites in a tokamak plasma spectrum

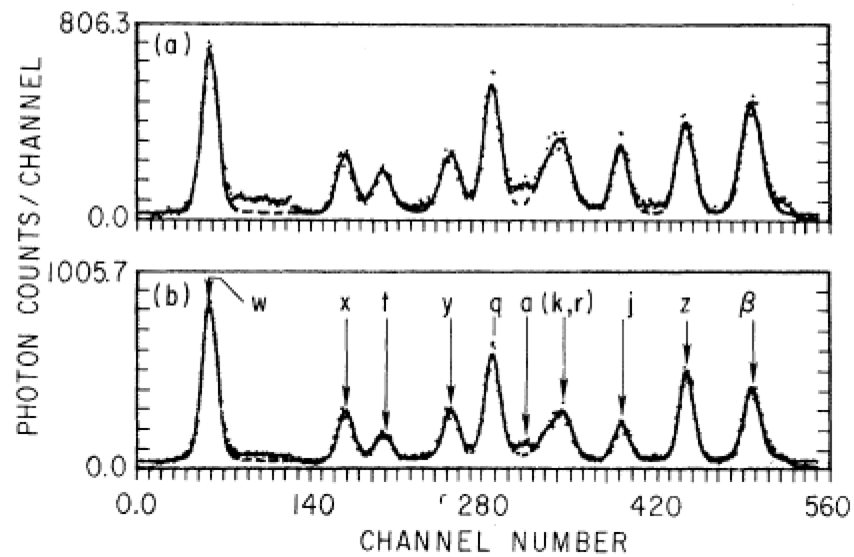


FIG. 1. (a), (b) Dielectronic satellite spectrum of Fe XXV as recorded by a multichannel analyzer from PLT for a central electron temperature of 1.65 and 2.30 keV, respectively. The photon energy decreases with

*Bitter et al. (Phys Rev Letts 1979)*

Tokamaks have been used as possible fusion machines – this is an Fe XXV/Fe XXIV X-ray spectrum from the Princeton Large Torus (PLT) in the USA. The densities are about 100 x more than solar flares but the temperatures are very similar (*T* approx. 25 MK).

# Emission measure & electron density

Emission measure is defined by

$$EM = \int_V N_e^2 dV$$

and is frequently used in solar X-ray astronomy. Very roughly, one can set EM = $N_e^2\, V$ where $V$ is the total volume of a flare, for example.

If there are images available from the *Hinode* XRT (X-ray Telescope), then one could obtain the electron density $N_e$.

In general, the densities obtained are lower limits, so the real densities may be higher.

# Electron densities from X-ray line ratios

It is quite easy to get temperatures from X-ray line ratios, but very few line ratios are sensitive to electron densities.

Some information is available from Fe XXI & Fe XXII lines which occur at about 12 Å.

A spectral scan of this region was made during a flare using the Flat Crystal Spectrometer (FCS) on *Solar Maximum Mission* (*SMM*) in 1980. The FCS had a fine collimator with a stepper motor to move seven different crystals on a rotatable shaft.

# Lines at 12 Å in FCS channel 2 (beryl crystal)

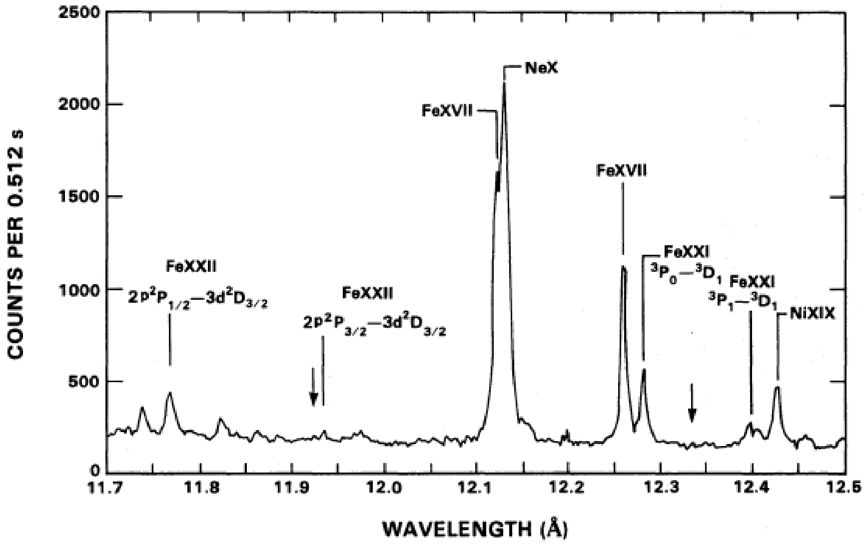


Several lines of Fe XXI and Fe XXII were visible during the decay of a flare in August 1980. They are all excited from the ground state of the Fe ions.

Two lines are predicted to occur at electron densities of more than $10^{12}$ cm$^{-3}$. They were not visible, so the electron density in this flare was evidently less than $10^{12}$ cm$^{-3}$.

# Element abundances

RESIK on *Coronas-F* is one of the best characterized spectrometers of all solar instruments – see Sylwester et al. (*Sol. Phys. 2005*).

This has enabled a program of element abundance determinations which have considerably refined earlier ones.

Our latest results (J. Sylwester, B. Sylwester, A. Kępa, KJHP and others) include the following:

| | *RESIK X-ray flares* | *Photospheric (Asplund)* |
|---|---|---|
| Si | 7.53 (.08) | 7.51 (.03) |
| S | 6.91 (.07) | 7.12 (.03) |
| Cl | 5.75 (.26) | 5.50 (.30) |
| Ar | 6.47 (.08) | 6.40 (.13)* |
| K | 6.06 (.34) | 5.03 (.09) |

* *photospheric proxies*

*Abundances logarithmic, H=12*

# Spectral line profiles

With crystal spectrometers, the crystals are never perfect – there is a “mosaic” of tiny sub-crystals in which the crystal planes are slightly misaligned.

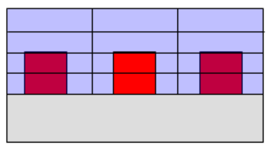

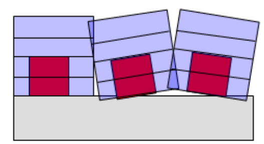

So instead of seeing a perfectly narrow line, one sees a broadened line with a line “profile”.

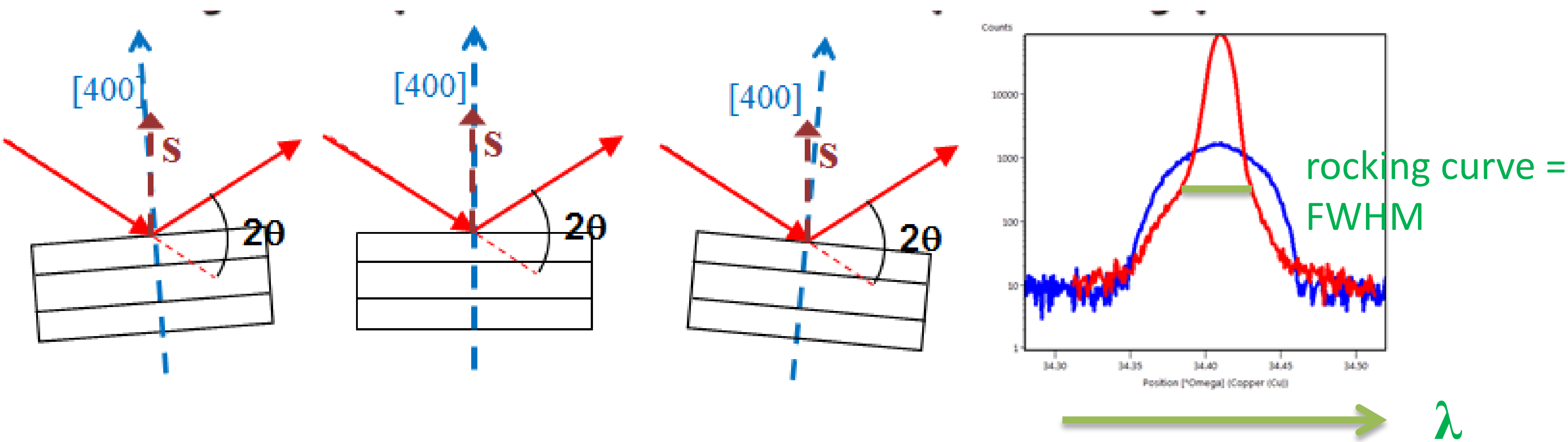

# Line profiles for solar flares

The rocking curve width is the FWHM in Å.

So crystals that have narrow rocking curves are best for examining solar X-ray flares.

This is crucial for the beginning of solar flares – the impulsive stage – when the line profiles are broadened and for disk flares there is a "blue" (short-wavelength) component. This means that there is a plasma component approaching the observer.

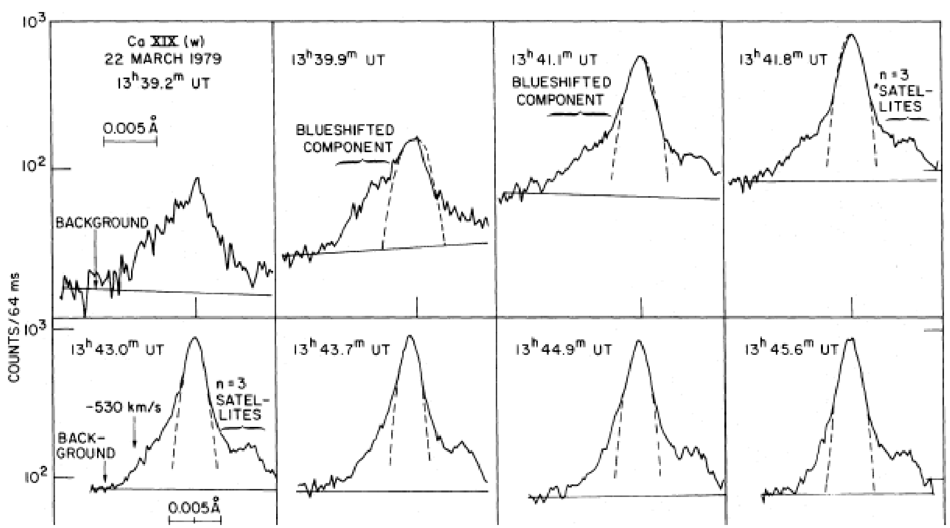


Ca XIX w line profiles in flare impulsive stage. *Feldman et al. (ApJ 1980)*

# De-convolving line profiles

Deconvolving observed line profiles by taking out the crystal rocking curves offers a much improved picture of solar X-ray spectra.

Listen to the next talk by Janusz Sylwester for some exciting new results being obtained for SMM spectra.

# Non-thermal electrons

It is likely that there are large numbers of non-thermal electrons at the flare impulsive stage – they give rise to hard X-ray pulses with durations of a few seconds.

There is a way of detecting them – using dielectronic satellites which sample the electron distributions at single energies.

For Fe XXIV satellites, some sample an electron distribution at energy = 4.7 keV, others with energy = 5.8 keV. The Fe XXV line w is excited by electrons with energy > 6.7 keV.

The ratio of the Fe XXIV satellites & the Fe XXV w line should be consistent with a thermal distribution.

If not, non-thermal electrons could be present.

Unfortunately lines are broadened at the flare impulsive stage.

*e distribution for T=20MK*

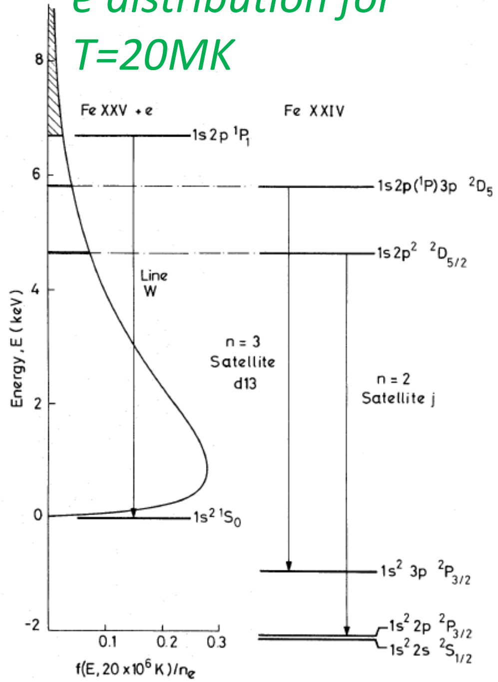

# Some results have been obtained.

Seely, Feldman, & Doschek (*ApJ 1987*) used P78-1 SOLFLEX spectra of the Fe XXV + Fe XXIV lines for some flares with hard X-ray bursts.

They used model electron distributions that appeared to give good agreement of the intensity ratios of the satellites & the Fe XXV w line, pointing to non-thermal distributions.

With improved spectra or looking at flares on the limb which have reduced amounts of line broadening, we might get more certain results.

Talks by Elena Dzifcakova and Alena Zemanova will give you much more information on this subject.

# X-ray continuum and instrumental background

X-ray continuum consists of free-bound (recombination) and free-free (bremsstrahlung) radiation. Neither dominates – they are comparable.

X-ray line-to-continuum ratios are a good way of measuring element abundances, for example Ca:

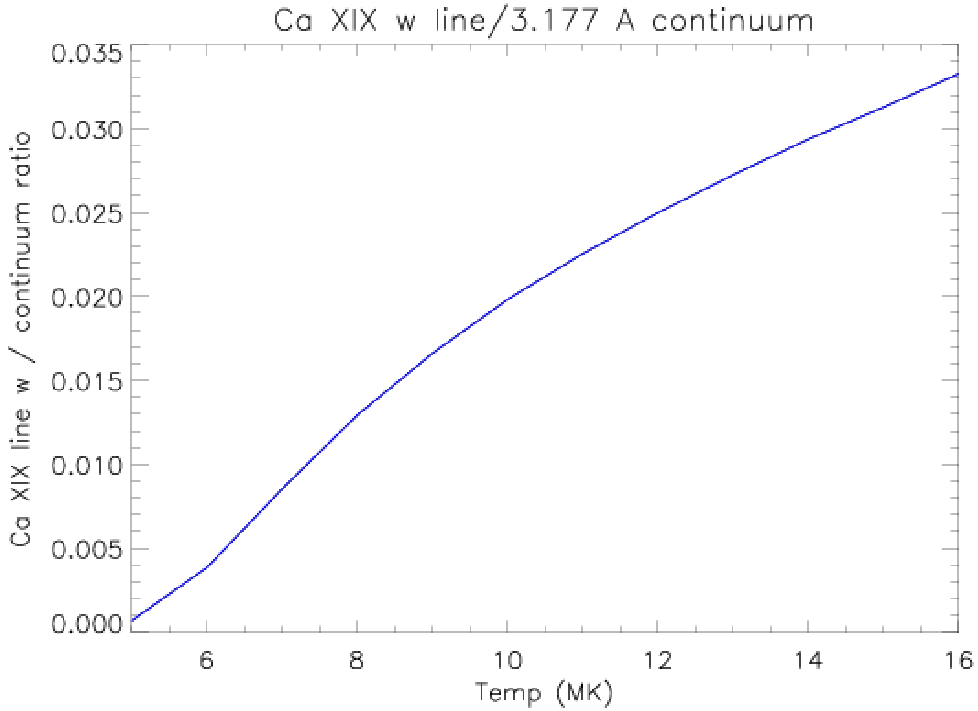

# Crystal spectrometers – background emission

When solar (or any) X-rays are incident on a crystal, the crystal material is liable to fluoresce.

Fluorescence is a process whereby the inner-shell (K-shell) electron is removed by an X-ray photon, the "hole" in the K-shell is filled by an electron in the M-shell to produce a Kα photon.

But a competing mechanism is for the atom to arrange itself with electrons successively filling holes with the excess energy carried away by an Auger electron.

Fluorescence radiation produces a background if X-rays are incident on a crystal, so crystal materials are chosen such that the fluorescence is small.

# What crystal material to use.

The probability of the radiative (K$\alpha$) transition occurring is called the fluorescent yield $\omega_K$ - it depends on the atomic number of the material. Roughly:

$$\omega_K = \frac{Z^4}{10^6 + Z^4}$$

(Z = atomic number).

For Fe, $\omega_K = 0.35$.

So to reduce the fluorescence background to a minimum, it is best to use crystals with very low atomic number. Commonly, LiF may be used. RESIK used Si and Quartz. However, the *SMM* BCS used germanium ($Z$=32), and the background was therefore high.

# Rejecting the background emission

The photons of the background emission may have a higher energy than the solar X-ray photons – this is true of the *SMM* BCS channel 1 which looked at Ca XIX lines (3.17 Å = 3.9 keV).

For Ge, the Kα photons have energy 9.85 keV.

So with the proportional counter detector on the BCS channel 1, pulse height discriminators could select only the low-energy photons (< 4 or 5 keV) and reject the Ge fluorescence photons with higher energy.

This was not so easy for the other BCS channels.

One could therefore look at the Ca XIX w line / continuum ratio in *SMM* flares to get a Ca abundance.

This was done by Sylwester et al. (1984 Nature, 1998 ApJ) to find a time-varying Ca abundance.

# Concluding Remarks

Solar X-rays have progressed enormously since the early days.

Instruments on spacecraft launched in the 1960s helped us to understand that there were extremely high temperatures in flare plasmas, up to Fe XXV (T= 25MK).

The more sophisticated spectrometers of the 1970s onwards, including RESIK (2001-2003), produced data that allow us to understand the physics of flare, active-region and quiet-Sun plasmas.

We now have much improved knowledge about flare flows, turbulence, element abundances, non-thermal electrons etc.

Future experimentation in the soft X-ray area includes ChemiX on the Russian *Interhelioprobe* spacecraft and SolPEX to be inserted in the Russian module of the *ISS*. Listen to talks by Marek Siarkowski and Marek Stęślicki.